

# Search for the Higgs boson in the $\gamma\gamma$ final state at the Tevatron

**Krisztian Peters**

**University of Manchester**

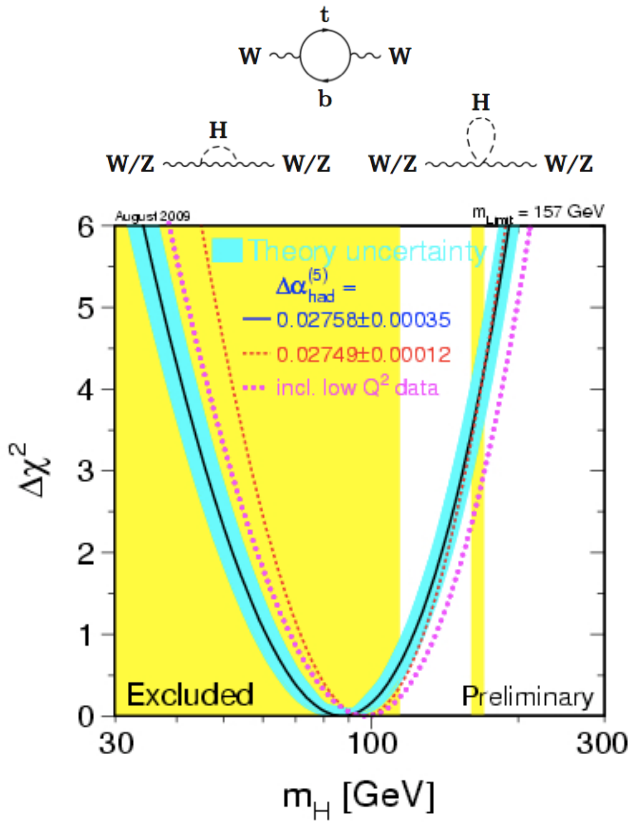
On behalf of the CDF and DØ collaborations

**23<sup>rd</sup> July 2010**

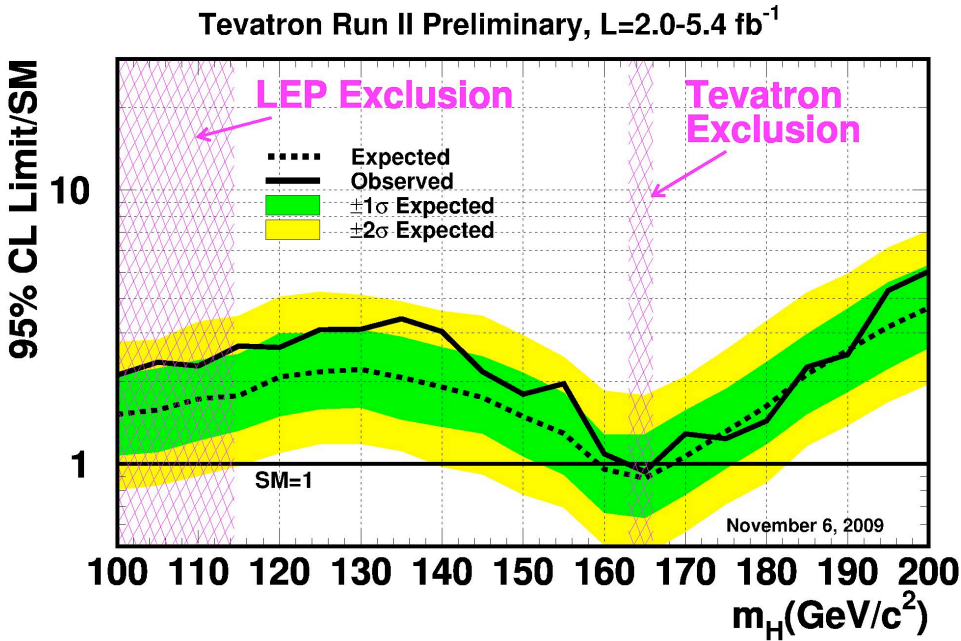
**35<sup>th</sup> Int. Conf. on High Energy Physics, Paris**



# Stalking the Higgs



## Combined Tevatron result 2009



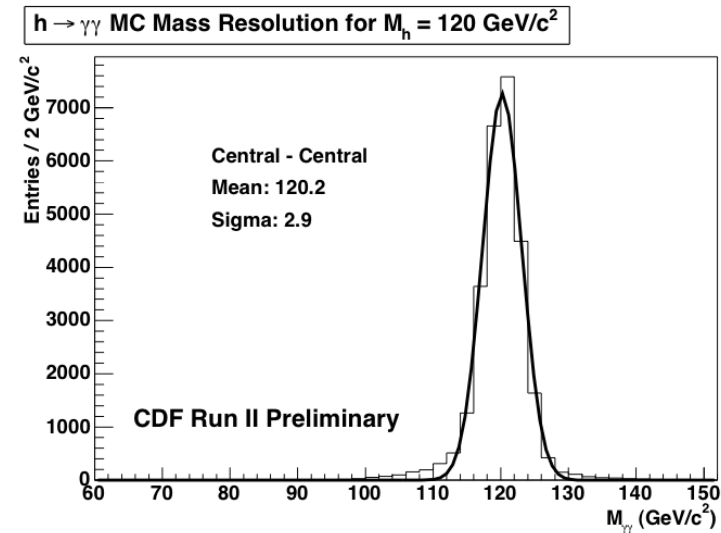
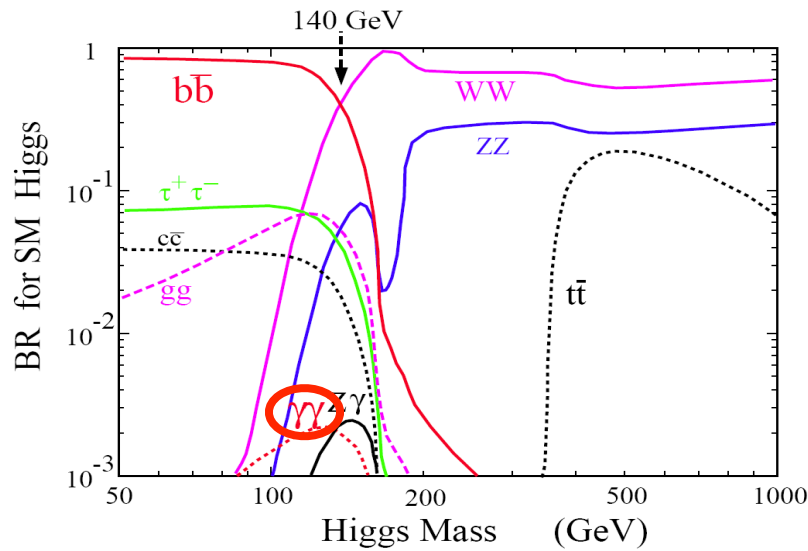
If the SM is correct, a light Higgs boson is around the corner!

Investigate different production mechanisms and a large number of final states to scan the whole mass range allowed at the Tevatron

# Why search for $H \rightarrow \gamma\gamma$ at the Tevatron?

Within the SM, small BR ( $\sim 0.2\%$ ) results in very small production rate

$\Rightarrow$  Compensate with much better mass resolution compared to dijet final states



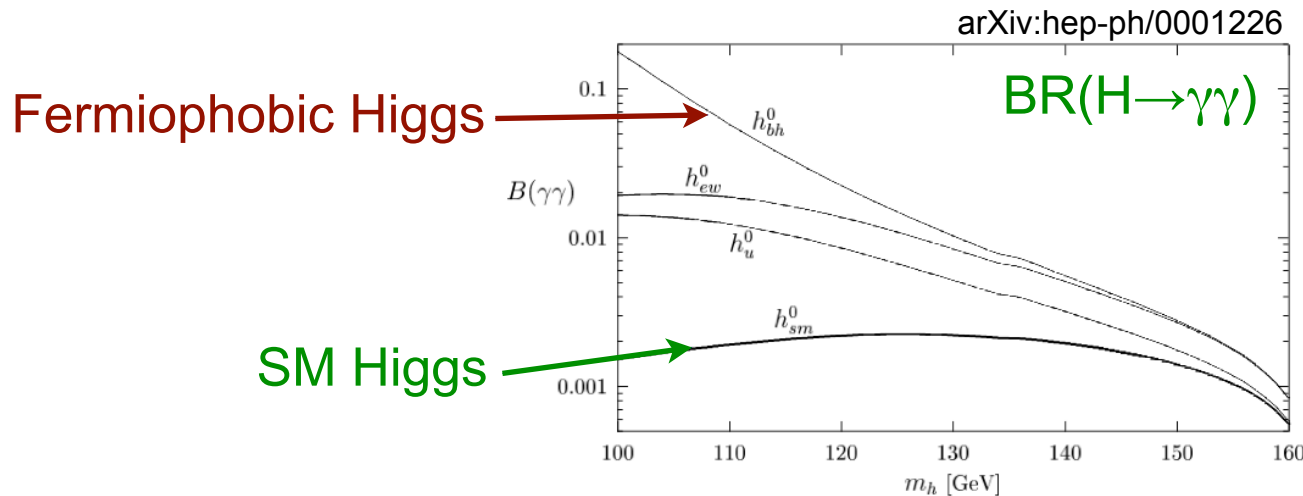
$H \rightarrow \gamma\gamma$  provides important additional sensitivity especially in the difficult intermediate mass region  $\sim 130 \text{ GeV}$

Forerunner to similar search at the LHC

# Why search for $H \rightarrow \gamma\gamma$ at the Tevatron?

Beyond the SM, significant enhancements to the production rate possible:

- New particles affecting the loop-mediated  $Hgg$  or  $H\gamma\gamma$  couplings
- Increased  $BR(H \rightarrow \gamma\gamma)$  in models with modified Higgs couplings to fermions
- Fermiophobic example: suppressed couplings to all fermions



Fermiophobic models can be probed with  $H \rightarrow \gamma\gamma$  at the Tevatron

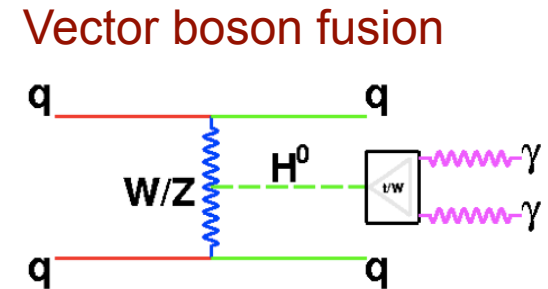
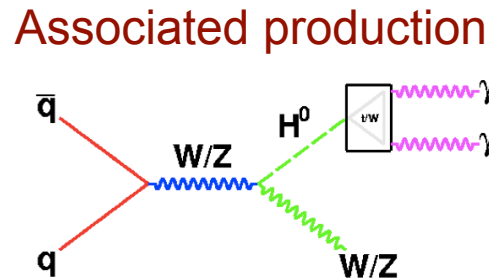
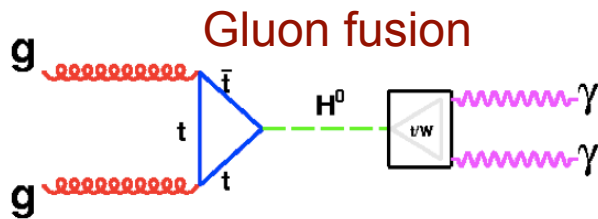
In general, this search can probe for any narrow resonance decaying into di-photons in a quasi-model independent way

# $H \rightarrow \gamma\gamma$ search at the Tevatron

Perform search as model-independent as possible

- Inclusive event selection
- Use only di-photon mass observable, look for bump in deeply falling spectrum
- Signal acceptance/sensitivity basically independent of production mechanism

For the Standard Model Higgs:

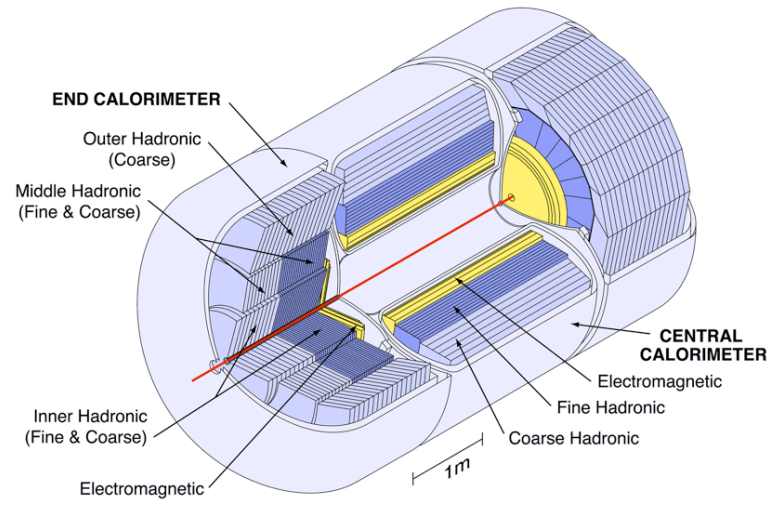
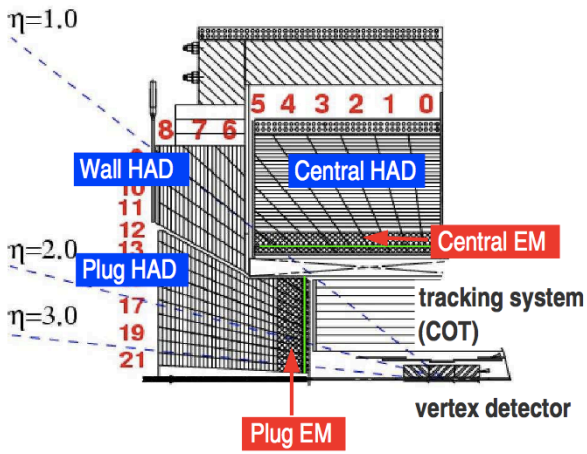


Add ~30% more signal

Relevant aspects for this search:

- Calorimeter resolution
- Photon identification
- Background model (data driven techniques)

# CDF and DØ calorimeters



## Central/Wall ( $|\eta| < 1.2$ ) and Plug calorimeters

- Scintillating tile with lead as absorber material in EM section
- Coarse granularity:  $\sim 800$  towers
- Nearly no noise
- EM resolution:  
 $\sigma/E = 13.5\% / \sqrt{E} \oplus 1.5\%$   
 (in central)

## Central ( $|\eta| < 1.1$ ) and forward calorimeters

- Liquid Argon with mostly uranium as absorber
- Fine granularity:  $\sim 50K$  cells
- EM resolution:  
 $\sigma/E = 21\% / \sqrt{E} \oplus 2.0\%$   
 (at normal incidence)

Both calorimeters calibrated regularly with special triggered data

# Photon energy scale and resolution

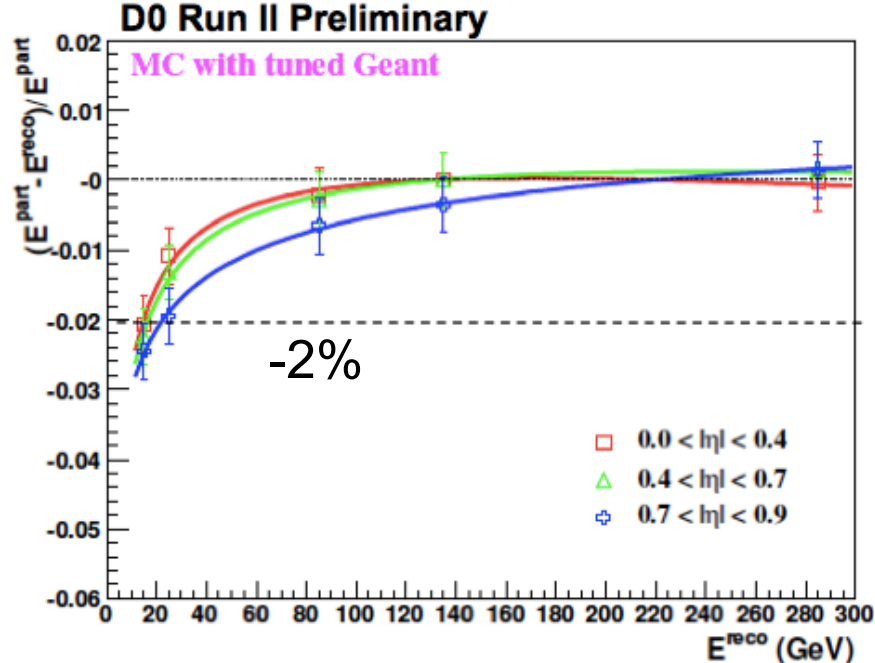
DØ example: the presence of additional dead material (non-uniformly distributed) with the Run II upgrade leads to:

- Shower maximum in frontal CAL layers
- Significant dependence of EM response and resolution on the particle energy and incident angle
- Different energy-loss corrections between electrons and photons

Energy-loss corrections measured in  $Z \rightarrow ee$  events. Propagated to different energy scales and photons with tuned GEANT simulation

Systematic uncertainties:

- Energy scale:  $\pm 0.5\%$
- Energy resolution:  $\pm 5\%$  in constant term

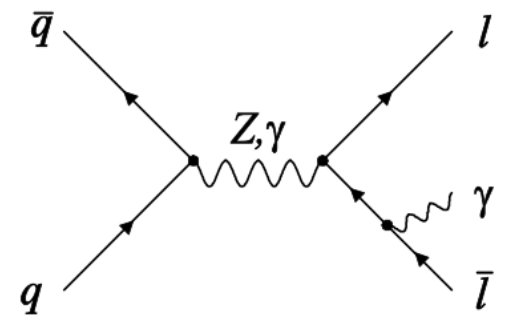
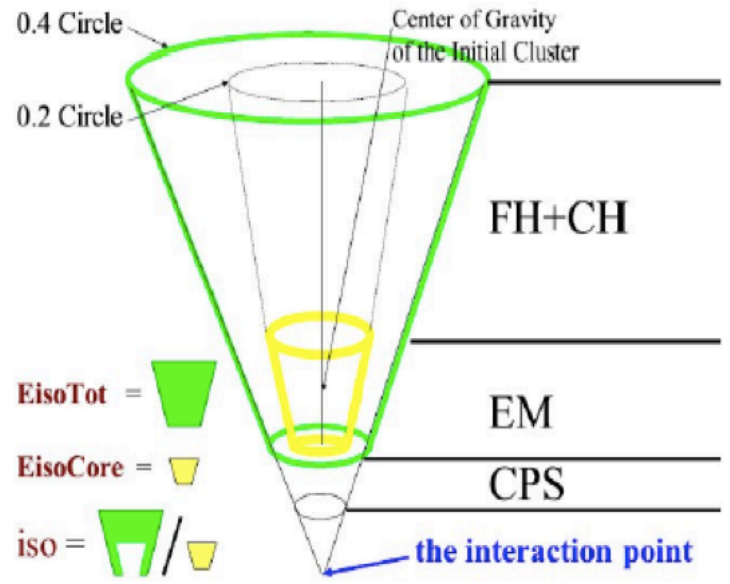


# Photon identification: basic selection

Both experiments select photons from EM clusters with the following criteria:

- High EM fraction / cluster in shower maximum detector
- Isolated in the calorimeter
- Isolated in the tracker
- Transverse shower profile consistent with EM object
- No associated track / no pattern of hits consistent with electrons

Differences between data and simulation calibrated using photons from radiative Z decays ( $Z \rightarrow l l \gamma$ ) and  $Z \rightarrow e e$

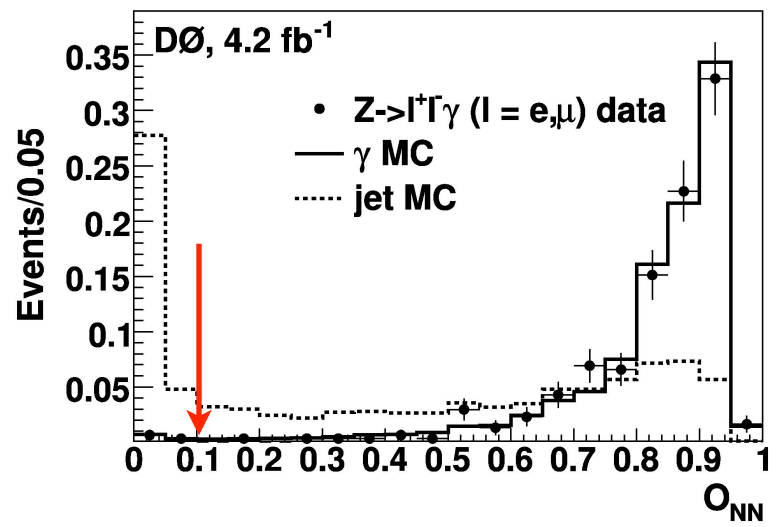
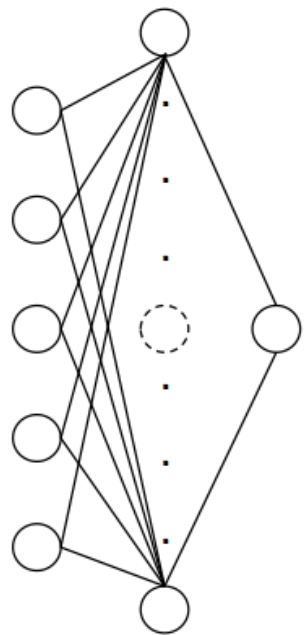




# Photon identification: Neural Network

DØ: Further improve photon purity with a five variable NN

- Tracker isolation ( $p_T^{\Sigma\text{trk}}$ )
- Number of EM1 cells within  $R<0.2$
- Number of EM1 cells  $0.2<R<0.4$
- Number of pre-shower clusters  $R<0.1$
- Energy-weighted width of energy deposition in the pre-shower detector



Trained using QCD  $\gamma\gamma$  and di-jet MC. Performance verified with Z → llγ data events - excellent agreement between data and MC

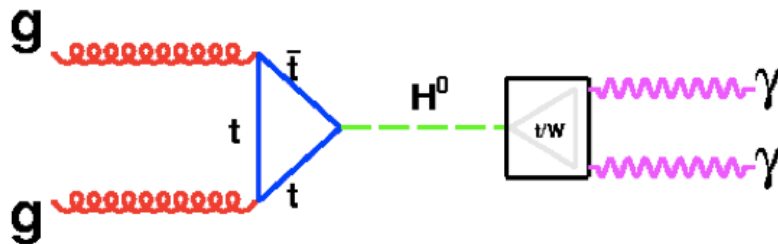
Require  $NN>0.1$  (almost 100% efficient for photons while rejecting 50% misidentified jets)

# Event selection

Data collected with a suite of calorimeter only triggers:

- Di-EM triggers ( $p_T$  thresholds vary within 12-25 GeV)
- Single photon triggers with high  $p_T$  threshold 50/70 GeV (CDF only)
- Trigger efficiency after offline selection  $\sim 100\%$

Require primary vertex within the acceptance of the tracking detectors



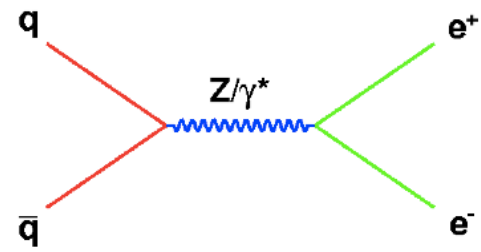
Two photons candidates:

- In central calorimeters (away from module boundaries)
- $p_T > 15 / 25$  GeV (CDF / DØ)
- $M_{\gamma\gamma} > 30 / 60$  GeV (CDF / DØ)

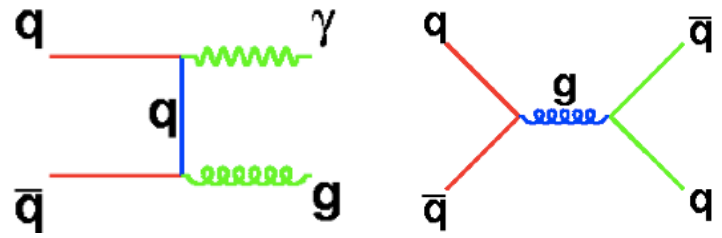
# Main backgrounds

## Reducible backgrounds:

Electrons misidentified as photons:  $Z/\gamma^* \rightarrow ee$   
Estimated using MC normalized to NNLO theoretical cross section

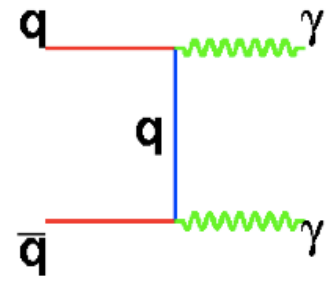


Jets misidentified as photons: di-jet and  $\gamma$ +jet  
Normalization and shape estimated from data



## Irreducible background:

Direct QCD di-photon production  
Normalization and shape estimated from data using sideband fitting method



In the CDF analysis the sum of all backgrounds is taken from an inclusive sideband fitting method

# Di-jet / $\gamma$ +jet background modeling

## 4x4 Matrix Method:

Use efficiency of a tighter cut ( $NN > 0.75$ ) to classify the events in 4 categories

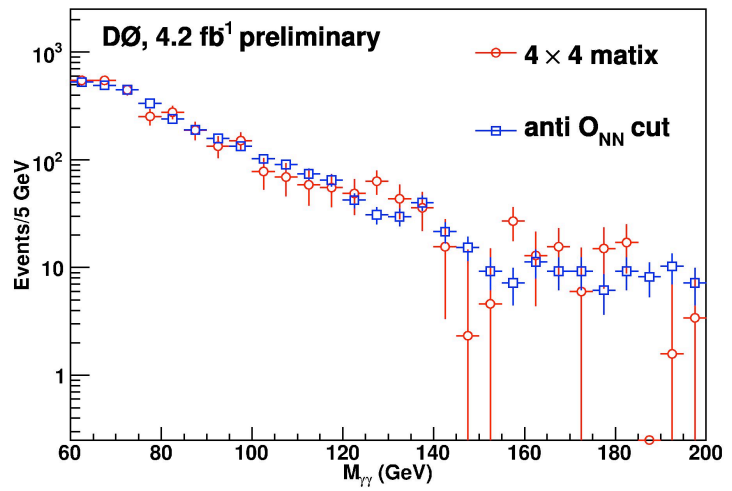
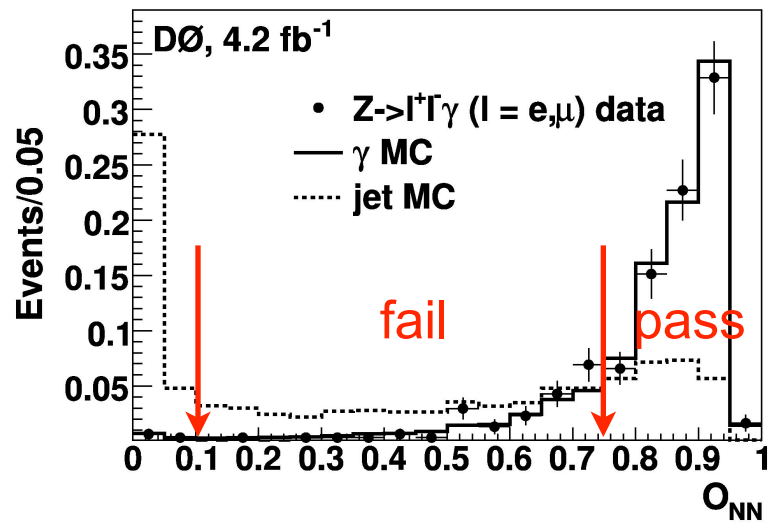
$$\begin{pmatrix} w_{jj} \\ w_{j\gamma} \\ w_{\gamma j} \\ w_{\gamma\gamma} \end{pmatrix} = E^{-1} \times \begin{pmatrix} w_{ff} \\ w_{fp} \\ w_{pf} \\ w_{pp} \end{pmatrix}$$

- Both photons fail
- Leading fail, trailing passes
- Leading passes, trailing fails
- Both photons pass

Solve linear equation with photon and jet efficiencies to obtain  $N_{jj} + N_{\gamma j} + N_{j\gamma}$

## Inverse-NN Method:

Invert NN (0.1) cut for one photon candidate to obtain enriched non- $\gamma\gamma$  sample from data



# Di-jet / $\gamma$ +jet background modeling

4x4 Matrix Method: **For normalization**

Use efficiency of a tighter cut ( $NN > 0.75$ ) to classify the events in 4 categories

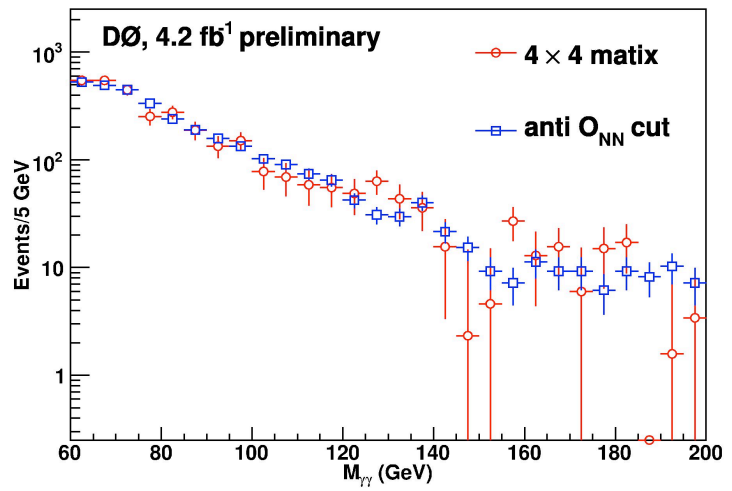
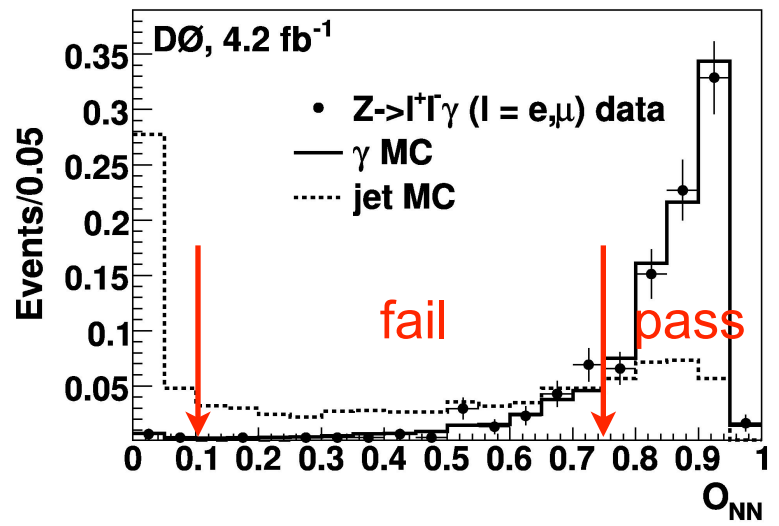
$$\begin{pmatrix} w_{jj} \\ w_{j\gamma} \\ w_{\gamma j} \\ w_{\gamma\gamma} \end{pmatrix} = E^{-1} \times \begin{pmatrix} w_{ff} \\ w_{fp} \\ w_{pf} \\ w_{pp} \end{pmatrix}$$

- Both photons fail
- Leading fail, trailing passes
- Leading passes, trailing fails
- Both photons pass

Solve linear equation with photon and jet efficiencies to obtain  $N_{jj} + N_{\gamma j} + N_{j\gamma}$

Inverse-NN Method: **For shape**

Invert NN (0.1) cut for one photon candidate to obtain enriched non- $\gamma\gamma$  sample from data



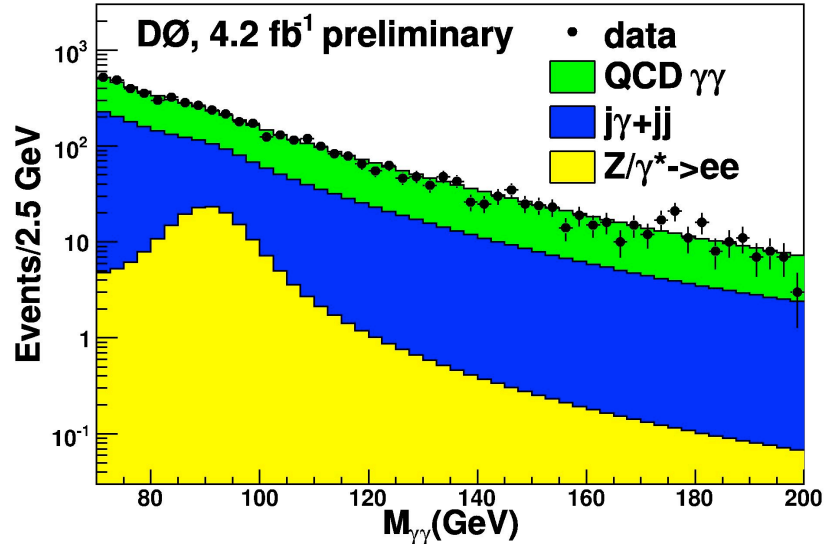
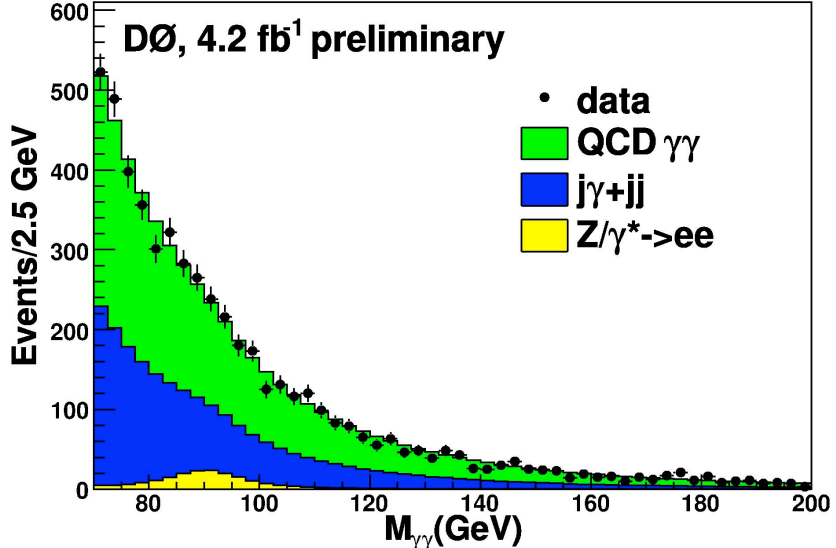
# Direct di-photon production

Challenging to predict theoretically. Estimated from sideband fitting in data after subtraction of the reducible backgrounds

Fitting range is [70,200] GeV, excluding the signal region, defined to be interval  $m_H \pm 15$  GeV

Choice of fitting function validated on PYTHIA reweighted to DIPHOX (NLO)

$$f(M_{diem}) = \exp(p_0 \cdot M_{diem}^2 + p_1 \cdot M_{diem} + p_2)$$



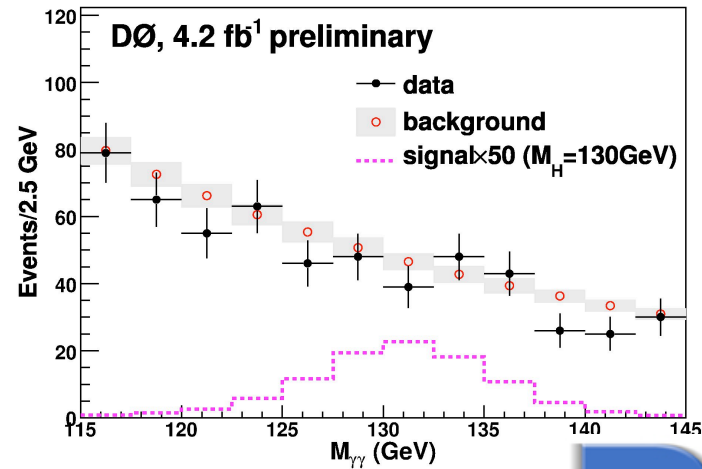
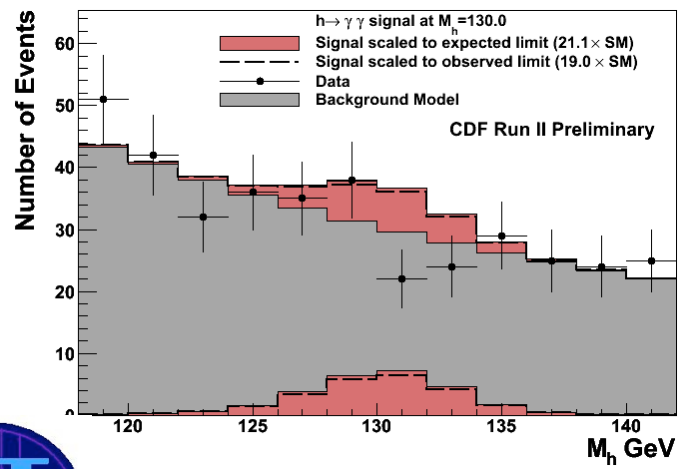
# Systematic uncertainties

Systematic uncertainties affecting the normalization and shape of the  $M_{\gamma\gamma}$  spectrum are estimated for both signal and backgrounds

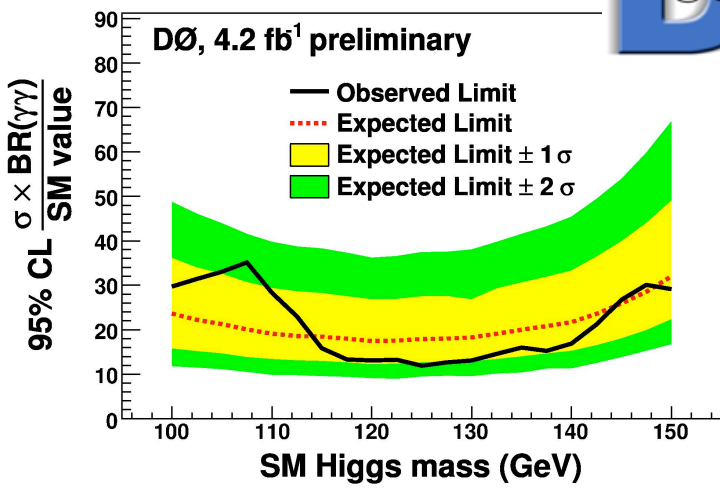
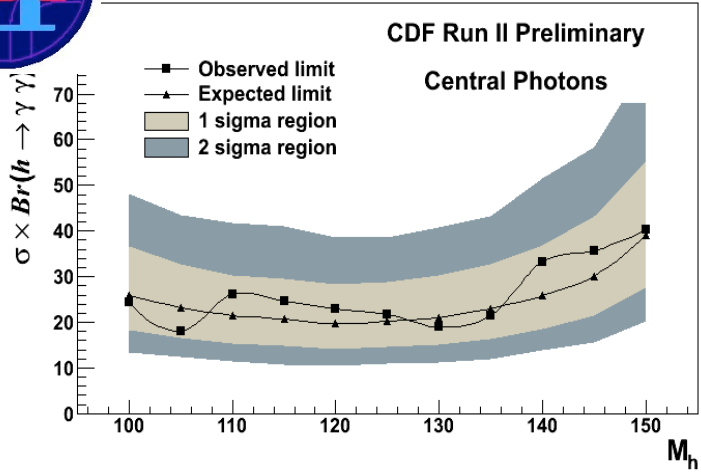
source	uncertainty
luminosity	6.1%
trigger	0.1%
PDF for $h \rightarrow \gamma\gamma$ acceptance	1.7% - 2.2%
electron misidentification efficiency	19.0%
$Z/\gamma^*(ee)$ cross section	3.9%
photon identification efficiency	6.8%
background subtraction	shape
photon energy scale	shape

Systematic uncertainties have small effect of limits, final sensitivity completely driven by statistics

# SM Higgs limits



Limits for  $h \rightarrow \gamma\gamma$  ( $5.4 \text{ fb}^{-1}$ )



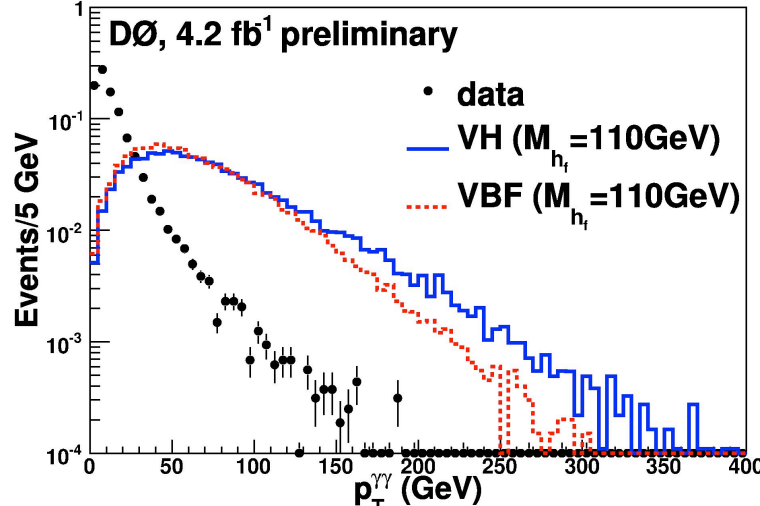
The  $M_{\gamma\gamma}$  spectrum in the search region is used to derive limits, which are a factor of  $\sim 20$  above the SM expectation for  $m_H = 100 \sim 140 \text{ GeV}$



# Fermiophobic Higgs limits

Large enhancement to  $BR(H \rightarrow \gamma\gamma)$

Gluc-fusion mechanism absent.  
Significant Higgs recoil in VH and VBF production

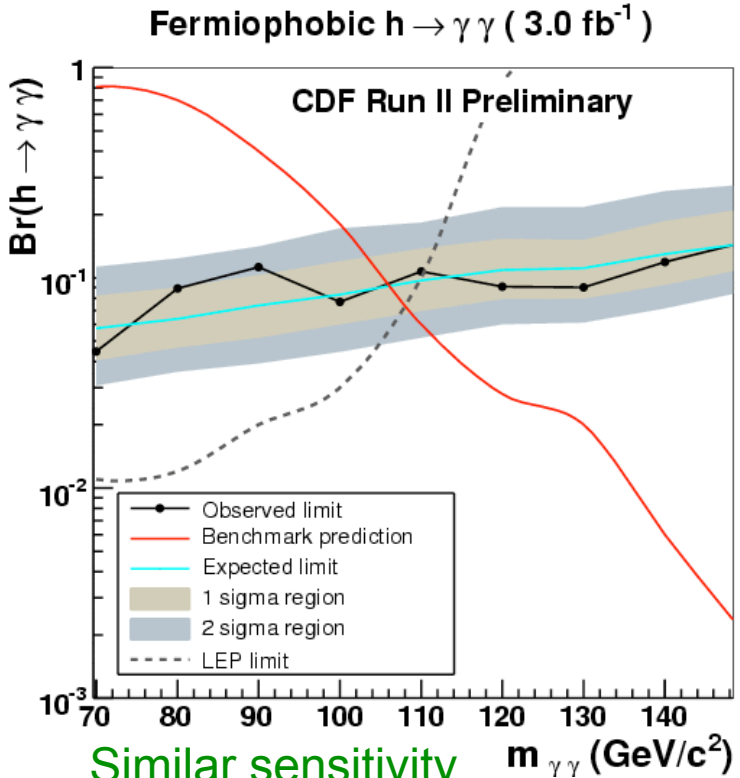


Similar to SM analysis, but require large di-photon  $p_T$ :

$$p_T(\gamma\gamma) > 75 / 35 \text{ GeV (CDF / DØ)}$$

Within Fermiophobic scenario, exclude  $m_H > 106 \text{ GeV}$

Probing BR beyond kinematic reach of LEP



Similar sensitivity for DØ analysis

# Conclusions

## SM Higgs:

Due to the good mass resolution for di-photons,  $H \rightarrow \gamma\gamma$  search adds  $\sim 5\%$  sensitivity to Tevatron's SM Higgs combination

- Especially important for the difficult intermediate mass region  $\sim 130$  GeV

Expect main improvements from multivariate analysis

- Di-photon differential cross-section measurements at the Tevatron tell how well the theory works and how to reweight the MC

## Fermiophobic Higgs:

Both Tevatron experiments have better sensitivity than any single LEP experiment

- Next round of results likely to exceed combined LEP result

Limits on  $BR(H \rightarrow \gamma\gamma)$  probing new territory beyond kinematic reach of LEP

